Journal of
MATERIALS RESEARCH



# Measuring the critical thickness of thin metalorganic precursor films

Ryan K. Roeder and Elliott B. Slamovich
*School of Materials Engineering, Purdue University, West Lafayette, Indiana 47907-1289*

(Received 5 August 1998; accepted 8 March 1999)

Successful application of sol-gel, metalorganic decomposition, or hydrothermal routes to ceramic thin films depends on the mechanical integrity of the precursor film. Above a critical thickness, a precursor film will crack or decohere from the substrate during drying. The cracking and thickness of thin metalorganic precursor films were simultaneously observed during drying using a standard optical microscope. Isochromatic color fringes produced by interference of reflected white light were used to monitor film thickness. The critical film thickness was determined by the color fringe corresponding to the thickness at which propagating cracks terminated. As a demonstration of the technique, the critical thickness of titanium di(isopropoxide) bis(ethyl acetoacetate) films was measured, showing increased critical thickness with the addition of small amounts of an elastomeric polymer.

Amorphous precursor thin films are converted into crystalline ceramic thin films by a variety of techniques, including sol-gel processing, metalorganic decomposition (MOD), and hydrothermal processing. In each of these methods, a substrate is first coated with a precursor film, usually by spin or dip coating. The precursor film is then dried and converted into a ceramic thin film by a chemical and/or thermal processing step. During each step, the film volume may decrease due to loss of volatile organics and increased film density. If the film adheres to the substrate, volume changes constrained in the plane of the substrate induce internal stresses which may cause film cracking.[1–7] Moreover, cracking of the precursor film consequently affects the mechanical integrity of the final ceramic film.

The mechanical integrity of thin films has long been observed to be dependent on film thickness. Above a critical thickness, brittle films under a tensile stress are observed to crack spontaneously or propagate cracks from preexisting flaws.[2–5] Cracking occurs when the strain energy release rate exceeds the film fracture toughness, or (in concept) when internal stresses exceed the cohesive strength of the film.[6–10] Films above a critical thickness can also decohere from the substrate when interfacial stresses exceed the adhesive strength.[8–11] The critical film thickness for cracking has typically been observed in the range 0.4–1.0 $\mu$m for a variety of materials and conditions.[2–6] These thicknesses are suitable for measurement by optical techniques.

Isochromatic color fringes produced by interference of reflected white light can be used to measure the thickness of transparent thin films in the micrometer-submicrometer range.[12,13] The major disadvantage of the technique is that the refractive index of the film must be known.[12,14] However, when the refractive index is known, the simplicity of the technique is a major advantage, requiring only a standard optical microscope. Furthermore, isochromatic color fringes on a thin film reveal a film thickness "contour map" that can be monitored as film cracking is observed. Other more sensitive optical techniques, such as ellipsometry and prism coupling, are not amenable to measuring thickness variations, or simultaneously observing film thickness and cracking behavior.[12–15]

In this study, the critical thickness of titanium di(isopropoxide) bis(ethyl acetoacetate) (TIBE) films was determined using isochromatic color fringes produced by interference of reflected white light. TIBE has been used to produce titanate thin films[16,17] and is known to be prone to cracking during drying.[17] Consequently, the effect of polymer additions on the critical thickness was examined, showing increased critical thickness for films with polymer additions and demonstrating the utility of the measurement technique.

TIBE is a commercially available (Gelest Inc., Tullytown, PA) metalorganic precursor, made by reacting titanium tetraisopropoxide with ethyl acetoacetone.[18] As-received TIBE was diluted to 50 vol% in toluene. Two other precursor solutions were prepared by dissolving 5.0 and 10.0 wt% (relative to the TIBE) of an elastomeric styrene-butadiene-styrene block copolymer (Kraton D1102C, Shell Oil Co., Belpre, OH) in the TIBE-50 vol% toluene solution. The viscosity of the as-received TIBE and each precursor solution was measured as a function of shear rate using a 0.8° cone and plate viscometer (Model LVTDT-IICP, Brookfield Engineering Laboratories, Inc., Stoughton, MA).

Precursor solutions were spun on reflective platinum coated glass substrates. Glass cover slides (18 × 18 × 0.2 mm) were ultrasonically cleaned in methanol,

 

followed by dc-sputtering of platinum. A stylus profilometer (alpha-step 200, Tencor Instruments, Mountain View, CA) was used to measure the thickness, 300 nm, and root mean squared roughness, 10 nm measured over a 400 $\mu$m range, of the Pt coating. Prior to spin coating, the substrates were washed with toluene and dried under flowing argon. Precursor solutions were pipetted onto the substrates and held to the spin coater (Headway Research Inc., Garland, TX) by vacuum. Spin coating was carried out at 5000 rpm for 15 s in a forced convection fume hood (Liberty Ind. Inc., E. Berlin, CT).

Precursor films were dried at room temperature and atmospheric pressure. The film morphology (including film thickness, crack initiation, crack growth, and crack arrest) was observed during drying using an optical microscope (Model BHS, Olympus Optical Co. Ltd., Tokyo, Japan). The numerical aperture of objective lenses was 0.13, 0.40, and 0.70 for total magnifications of 50, 200, and 500×, respectively. The top surfaces of films were photographed periodically, up to 90 h after spin coating, using a standard 35 mm camera attached to the optical microscope. After 90 h drying, no significant morphological changes were observed.

Isochromatic color fringes were produced by interference of reflected white light in the precursor thin film.[12,19–21] Rays from a source of white light (standard optical microscope) were incident normal to the surface of precursor films on reflective Pt-coated glass substrates. Since the precursor films were transparent, light waves were reflected from the film surface and refracted upon entering the film. Light waves that entered the film were reflected from the substrate and refracted again upon leaving the film. Thus, a path difference existed between light waves reflected off the film and the substrate. Since the refractive index, $n$, increased from air ($n = 1.000$[19–21]) to the precursor film (TIBE, $n = 1.522$[22]) to the substrate (Pt, $n > 2$[12,20]), an additional one-half wavelength phase shift occurred for reflections at each interface.[12] For this case, the optical path difference (or retardation, $R$) for constructive interference of light waves was

$$R = 2nh = m\lambda, \tag{1}$$

where $n$ is the refractive index of the film, $h$ is the film thickness, $m$ is the wave order, and $\lambda$ is the wavelength of the color of light observed. Destructive interference occurred when the retardation of light waves was equal to $m - 1/2$ of their wavelength. As the film thickness varied, the retardation changed such that light waves of different wavelength (or color) constructively and destructively interfered. Also, the vividness of color fringes decreased with increased film thickness because fringes of increased wave order experienced increased destructive interference. For $m > 5$, fringes became faint and eventually invisible, preventing use of the technique. Abbreviated derivations of Eq. (1) are outlined in Refs. 12 and 19–21.

Film thickness was determined using Eq. (1) and the observed isochromatic color fringes. Direct calculation of the film thickness at a particular color fringe using $2nh = m\lambda$ was unrealistic because a single wavelength must be specified for the observed color fringe. A single color of light actually contains a range of wavelengths with an intensity maximum at the wavelength typically specified for that color. The ranges of wavelength for different colors can overlap, producing color combinations.[21] Furthermore, the sensitivity of the human eye varies for different colors.[21] These problems were circumvented by using retardations, $R$, tabulated for the color fringes commonly observed in various optical interference phenomena.[21,23,24] Thus, the known retardation for a particular color fringe was used to determine the film thickness for that color fringe according to Eq. (1), $R = 2nh$. The refractive index for TIBE, $n = 1.522$,[22] was used in all thickness measurements.

The average thickness of precursor films was dependent on the precursor solution viscosity. The viscosity measured for each precursor solution decreased with increasing shear rate from 1 to 10 $s^{-1}$, becoming constant from 10 to 1000 $s^{-1}$. Since spin coating was carried out at 5000 rpm, the relevant solution viscosity was the limit approached with increasing shear rate. The precursor solution viscosity measured above 10 $s^{-1}$ was 32 mPa s for the as-received TIBE, 3 mPa s for the TIBE–50 vol% toluene solution, 13 mPa s with 5.0 wt% polymer, and 26 mPa s with 10.0 wt% polymer. The above measurements were initial, lower bound solution viscosities, because in practice the solvent evaporated during spin coating. Note the decrease in TIBE viscosity with dilution in 50 vol% toluene, and the subsequent increase in TIBE–50 vol% toluene viscosity with polymer additions. After spin coating, the average film thickness increased with increasing initial solution viscosity, as observed qualitatively by color fringes (e.g., Fig. 1). The observed trend agrees with previous experimental and theoretical work showing a directly proportional relationship between the initial film thickness ($h_i$) and solution viscosity ($\eta$) ($h_i \propto \eta^{\alpha}$, where $\alpha = 1/3 - 1/2$[25–30]). The order of increasing average film thickness among the precursor solutions remained the same as the films dried.

Film cracking and thickness were simultaneously observed during drying. Observations of the as-received TIBE and TIBE–50 vol% toluene films after drying for 1 h showed that cracks initiated and grew radially from the thickest regions of the film. Cracks initiated at heterogeneities such as dust particles embedded in the film, which caused a localized increase in the film thickness above the critical film thickness. Propagation and bifurcation of the initial cracks resulted in the

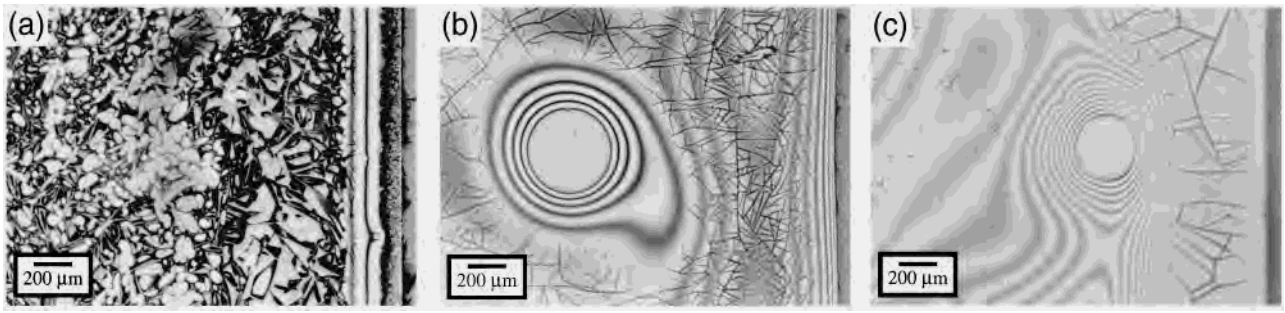


FIG. 1. Optical micrographs of films made from the (a) TIBE–50 vol% toluene solution with (b) 5.0 wt% and (c) 10.0 wt% (relative to TIBE) polymer after drying 90 h, showing differences in the cracking and decohesion of films. Note that the substrate edge is located on the right side of the micrographs.

formation of crack networks after 1.5 to 2 h. By 4 h, cracks had propagated throughout the majority of the film, and the film began to decohere from the substrate in the thickest regions. After 90 h, most of the film had decohered from the substrate [Fig. 1(a)]; however, crack arrest was observed in the thinnest regions of the film, corresponding to the outermost edges of the substrate (right side of micrograph) and the periphery of wetting flaws [voids in the film coverage, e.g., center of Fig. 1(b)]. Films made from TIBE–50 vol% toluene solutions with polymer additions still cracked, but did not decohere [Figs. 1(b) and 1(c)]. More importantly, cracking was suppressed in films with added polymer, despite increased film thickness, as shown by color fringes in Fig. 1. In the case of films with 10.0 wt% polymer, cracks were observed only in the thickest regions of the film and many cracks that had initiated were unable to grow [Fig. 1(c)]. Note that the extensive film cracking observed near the substrate edge in Fig. 1 was due to a meniscus resulting from spin coating. The meniscus was typically several times greater in film thickness than the larger and more uniform center region of the film shown on the left side of the micrographs.

The critical film thickness was determined after 90 h drying from higher magnification micrographs taken at the substrate edge (Fig. 2) and the periphery of wetting flaws, where cracks that had initiated in thicker film regions arrested while propagating into thinner regions. The critical thickness was defined as the film thickness below which cracks neither initiated nor propagated, and was measured by determining the film thickness at which propagating cracks terminated. An isochromatic color fringe chart was determined from known retardations for observed color fringes, using Eq. (1) and the refractive index for TIBE to calculate corresponding film thicknesses (Table I). The observed fringe color, fringe order, and measured critical film thickness for films of each precursor solution are tabulated in Table II. As shown in Fig. 2 and Table II, the critical film thickness for cracking increased with increasing polymer content. Since films processed from the as-received TIBE and TIBE–50 vol% toluene solutions exhibited the same critical thickness, the initial film thickness had no apparent influence on the measured critical film thickness. Note that the values reported in Table II are for the lowest critical thickness observed in each film, and may not exactly correspond to the micrographs shown in Fig. 2.

Errors associated with the optical interference technique were accounted for in the critical thickness results given in Table II. The following assumptions were made in the film thickness measurements of this study: (i) no light absorption by the film or substrate (phase shift on reflections of 0 or $\lambda/2$); (ii) constant film refractive index

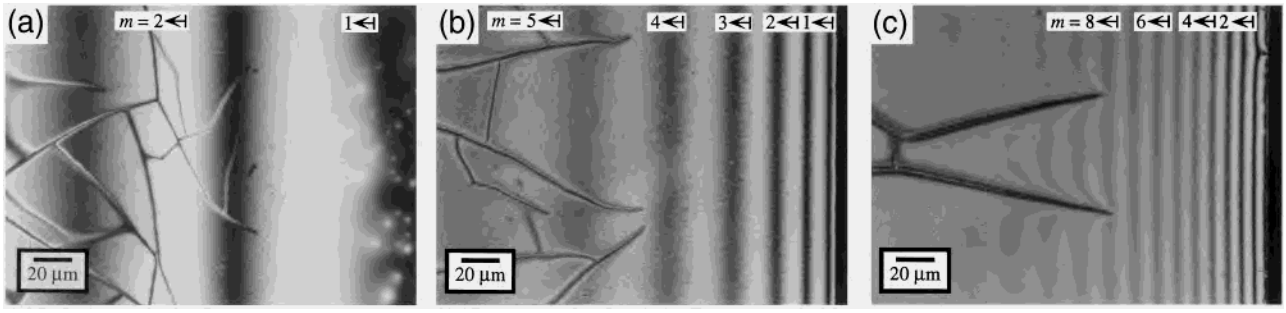


FIG. 2. Optical micrographs of films made from the (a) TIBE–50 vol% toluene solution with (b) 5.0 wt% and (c) 10.0 wt% (relative to TIBE) polymer after drying 90 h, showing crack termination at color fringes corresponding to the critical film thickness. The approximate wave order ($m$) of the color fringes shown in black and white is given as a guide for Table II. Note that the substrate edge is located on the right side of the micrographs.

TABLE I. Abbreviated isochromatic color fringe chart calculated for TIBE ($n = 1.522$[22]).

| $m$ | Color fringe | Retardation (nm) | Thickness ($\mu$m) |
|---|---|---|---|
| 1 | Black | 0 | 0.000 |
| | Gray blue | 160 | 0.053 |
| | White | 260 | 0.085 |
| | Yellow | 330 | 0.108 |
| | Yellow Brown | 440 | 0.145 |
| | Orange red | 500 | 0.164 |
| | Red | 540 | 0.177 |
| 2 | Violet | 580 | 0.191 |
| | Blue | 680 | 0.223 |
| | Blue green | 720 | 0.237 |
| | Green | 750 | 0.246 |
| | Yellow green | 840 | 0.276 |
| | Yellow | 920 | 0.302 |
| | Orange red | 1000 | 0.329 |
| | Violet red | 1050 | 0.345 |
| 3 | Blue green | 1250 | 0.411 |
| | Green | 1350 | 0.443 |
| | Yellow green | 1400 | 0.460 |
| | Yellow | 1450 | 0.476 |
| | Rose red | 1500 | 0.493 |
| | Carmine | 1550 | 0.509 |
| 4 | Blue gray | 1700 | 0.558 |
| | Blue green | 1750 | 0.575 |
| | Green brown | 1800 | 0.591 |
| | Pale green | 1900 | 0.624 |
| | Pale gray | 2000 | 0.657 |
| | Pale red Violet | 2200 | 0.723 |
| 5 | Pale green | 2500 | 0.821 |
| | Pink | 2700 | 0.887 |
| And so on... | | | |

with time, radiation wavelength, and polymer addition; and (iii) light incident normal to the film surface. Errors due to (i) and (ii) should be relatively small for the visible spectrum of light in the present system. Note that the refractive index for a styrene-butadiene-styrene block copolymer, $n = 1.534-1.535$,[31] is only $\approx 1\%$ higher than the refractive index for TIBE. The error due to (iii) generally increases with magnification, due to an increasing numerical aperture for an objective lens of increasing strength. Errors of this type are generally on the order of several percent (i.e., numerical aperture of 0.4–0.8), and can be as high as 10% of the measured thickness under extreme conditions (e.g., numerical aperture of 0.9 with a large aperture diaphragm).[32] Measurements made in this study were confirmed at the lowest magnification possible. Thus, the thickness measurements in this study are believed to be within several percent of the actual film thickness.[12,13] As a final note, the possibility of human error in distinguishing color fringes can be eliminated by employing a spectrophotometer,[33–35] but will compromise the simplicity of the above method.

The optical interference technique used in this study provided a simple means to simultaneously observe film thickness and cracking during drying. Furthermore, thin film fracture toughness, which is relatively unknown for most technologically significant thin film materials (including metalorganic precursors), is related to the critical film thickness.[8,9] Thus, by combining this technique with measurement of the strain or stress[36–40] in the film during drying, assessment of thin film fracture toughness could be made.[41]

## ACKNOWLEDGMENT

This research was supported by the National Science Foundation Grant DMR-9623744.

## REFERENCES

1. S. G. Croll, J. Appl. Polym. Sci. **23**, 847–858 (1979).
2. C. J. Brinker, A. J. Hurd, P. R. Schunk, G. C. Frye, and C. S. Ashley, J. Non-Cryst. Solids **147–148**, 424–436 (1992).
3. A. Atkinson and R. M. Guppy, J. Mater. Sci. **26**, 3869–3873 (1991).
4. S-Y. Chen and I-W. Chen, J. Am. Ceram. Soc. **78** (11), 2929–2939 (1995).
5. S. Bec, A. Tonck, and J-L. Loubet, in *Thin Films: Stresses and Mechanical Properties IV*, edited by P. H. Townsend, T. P. Weihs, J. E. Sanchez, Jr., and P. Børgesen (Mater. Res. Soc. Symp. Proc. **308**, Pittsburgh, PA, 1993), pp. 577–582.
6. K. Sato, Progr. Org. Coat. **8**, 143–160 (1990).
7. G. P. Bierwagon, J. Coat. Technol. **51** (658), 117–126 (1979).
8. A. G. Evans, M. D. Drory, and M. S. Hu, J. Mater. Res. **3**, 1043–1048 (1988).
9. M. S. Hu and A. G. Evans, Acta Metall. **37** (3), 917–925 (1989).
10. M. D. Thouless, Thin Solid Films **181**, 397–406 (1989).
11. S. G. Croll, J. Coat. Technol. **52** (665), 35–43 (1980).
12. O. S. Heavens, *Optical Properties of Thin Solid Films* (Butterworths Scientific Publications, London, 1955).
13. W. van Vonno, *Measurement of the Thickness and Refractive Index of Evaporated Dielectric Films* (Uitgeverij Waltman, Delft, 1968).

TABLE II. Critical thickness measured for TIBE precursor films.

| Solvent | Polymer[a] (wt%)[b] | Nearest observed fringe color | Fringe order, $m$ | Critical thickness, $h_c$ ($\mu$m) |
|---|---|---|---|---|
| None | 0.0 | Yellow | 1 | $0.10 \pm 0.01$ |
| 50 vol% toluene | 0.0 | Yellow | 1 | $0.11 \pm 0.01$ |
| 50 vol% toluene | 5.0 | Red | 3 | $0.51 \pm 0.05$ |
| 50 vol% toluene | 10.0 | Pink/pale green | 5/6 | $0.92 \pm 0.09$ |

[a]Kraton D1102C, a styrene-butadiene-styrene block copolymer.
[b]Added in wt% relative to the precursor.

14. A. C. Adams, D. P. Schinke, and C. D. Capio, J. Electrochem. Soc. **126** (9), 1539–1543 (1979).
15. R. Ulrich and R. Torge, Appl. Opt. **12** (12), 2901–2908 (1973).
16. E. B. Slamovich and I. A. Aksay, J. Am. Ceram. Soc. **79** (1), 239–247 (1996).
17. E. B. Slamovich and I. A. Aksay, in *Better Ceramics Through Chemistry VI*, edited by A. K. Cheetham, C. J. Brinker, M. L. Mecartney, and C. Sanchez (Mater. Res. Soc. Symp. Proc. **346**, Pittsburgh, PA, 1994), pp. 63–68.
18. A. Yamamoto and S. Kambara, J. Am. Chem. Soc. **79**, 4344–4348 (1957).
19. J. E. Greivenkamp, in *Handbook of Optics*, 2nd ed., edited by M. Bass (McGraw-Hill, New York, 1995), Vol. 1, pp. 2.3–2.25.
20. M. Born and E. Wolf, *Principles of Optics*, 4th ed. (Pergamon Press, Oxford, 1970).
21. K. Nassau, *The Physics and Chemistry of Color* (John Wiley and Sons, New York, 1983).
22. Personal communication, Gelest Inc., Tullytown, PA.
23. R. B. Heywood, *Photoelasticity for Engineers* (Pergamon Press, Oxford, 1969).
24. G. C. Mönch, Optik **9**, 75–83 (1952).
25. C. Extrand, Polym. Eng. Sci. **34** (5), 390–394 (1994).
26. W. A. Levinson, A. Arnold, and O. DeHodgins, Polym. Eng. Sci. **33** (15), 980–988 (1993).
27. A. Weill and E. Dechenaux, Polym. Eng. Sci. **28** (15), 945–948 (1988).
28. D. E. Bornside, C. W. Macosko, and L. E. Scriven, J. Electrochem. Soc. **138** (1), 317–320 (1991).
29. D. Meyerhofer, J. Appl. Phys. **49** (7), 3993–3997 (1978).
30. A. G. Emslie, F. T. Bonner, and L. G. Peck, J. Appl. Phys. **29** (5), 858–862 (1958).
31. *Polymer Handbook*, edited by J. Brandrup and E. H. Immergut (John Wiley and Sons, New York, 1989).
32. W. A. Pliskin and R. P. Esch, J. Appl. Phys. **39** (7), 3274–3276 (1968).
33. E. A. Corl and H. Wimpfheimer, Solid-State Electron. **7**, 755–761 (1964).
34. F. Reizman, J. Appl. Phys. **36** (12), 3804–3807 (1965).
35. F. Reizman and W. van Gelder, Solid-State Electron. **10**, 625–632 (1967).
36. J. H. L. Voncken, C. Lijzenga, K. P. Kumar, K. Keizer, A. J. Burggraaf, and B. C. Bonekamp, J. Mater. Sci. **27**, 472–478 (1992).
37. S. Lampenscherf and W. Pompe, Z. Metallkd. **89** (2), 96–105 (1998).
38. K. E. Boggs, D. L. Wilcos, D. A. Payne, and L. S. Allen, *Proc. SPIE Int. Soc. Opt. Eng.* **2256**, 350–355 (1994).
39. R. C. Chiu and M. J. Cima, Ceram. Trans. **22**, 347–356 (1991).
40. T. J. Garino and M. Harrington, in *Ferroelectric Thin Films II*, edited by A. I. Kingon, E. R. Myers, and B. Tuttle (Mater. Res. Soc. Symp. Proc. **243**, Pittsburgh, PA, 1992), pp. 341–347.
41. R. K. Roeder and E. B. Slamovich, Ceram. Trans. **83**, 375–382 (1998).